*Proceedings of the 11th Brazilian Congress of Thermal Sciences and Engineering -- ENCIT 2006*
*Braz. Soc. of Mechanical Sciences and Engineering -- ABCM, Curitiba, Brazil,- Dec. 5-8, 2006*

**Paper CIT06-1007**

# STABILITY ANALYSIS OF SLIGHTLY-INCLINED STRATIFIED OIL-WATER FLOW AND INTERMEDIATE WAVE THEORY

**Oscar M.H. Rodriguez**
Department of Mechanical Engineering, University of São Paulo at São Carlos (EESC-USP), Brazil
oscarmhr@sc.usp.br

**Robert F. Mudde**
**René V.A Oliemans**
J.M. Burger Centre for Fluid Mechanics, Kramers Laboratorium, Delft University of Technology (TUDelft), The Netherlands

***Abstract.*** *A general transition criterion is being proposed in order to locate the stratified flow pattern in horizontal and slightly inclined oil-water flow. The criterion proposed is based on the one-dimensional two-fluid model of liquid-liquid two-phase flow. It considers the existence of a critical wave length related to a non-negligible interfacial tension term for which the linear stability theory still applies. Hence, the neutral-stability wave number is no longer set to zero. Furthermore, it is shown that the common assumption of unitary shape factors is lacking. The long wave approximation is no longer applied, hence a new destabilizing term related to the cross-section curvature of the interface is derived. A new closure relation for the interfacial shear stress is suggested for the two-fluid model for stratified pipe flow and improvements in the pressure loss predictions are presented. The proposed transition boundary is compared with three different models from the literature. New experimental data (setup of length 15.5 m and diameter 8.28 cm at various slightly inclined orientations) on oil-water interfacial wave are presented. The good agreement between theory and data is promising.*

***Keywords.*** *Two-phase flow, Oil-water flow, Stratified flow, Stability analysis, Closure relations, Experimental data*

## 1. Introduction

Production logging is one of the most important aspects of managing oil/gas production of a field. It provides insight into the type and rates of fluid flow in the reservoir, which is critical to optimizing the life of the well. In multiphase oil/gas production logging analysis one would like to derive, from limited down-hole information on pressure loss and phase holdup, the oil and water production rates one can expect in tubing at angles from horizontal up to vertical. A flow pattern dependent model has been chosen as modelling approach, since for the gas-liquid flow it has proven to be the most reliable method to calculate two-phase pressure gradient and holdup. It has been shown recently that in horizontal flow it is possible to correlate holdup and pressure gradient measurements with relatively small ranges of oil and water superficial velocities via an inverted mode of flow pattern dependent method (Rodriguez *et al.* 2004, Guet *et al.* 2006).

Several methods for calculating the pressure drop and the volumetric fractions of the phases in pipelines have been presented, which require a correct prediction of the flow patterns (Nädler and Mewes, 1997, Angeli and Hewitt, 1998, Rodriguez and Oliemans, 2006). Observations of the many known kinds of liquid-liquid flow patterns in a single apparatus depend on the fluid properties, pipe size and geometry involved (Charles *et al.*, 1961, Trallero, 1995, Flores *et al.*, 1997, Valle and Utvik, 1997, Sotgia and Tartarini, 2001, Lovick and Angeli, 2001 and 2004, Bannwart *et al.*, 2004). Some studies have been carried out on oil-water flow in large and/or inclined pipes. Alkaya *et al.* (2000) experimentally investigated the effect of the inclination angle on flow pattern transition boundaries in a slightly inclined 5 cm i.d. pipe (from –5º to +5º, from the horizontal). Although those authors reported the existence of high-amplitude interfacial waves in inclined flow, they did not differ stratified with mixing at the interface flow pattern from stratified wavy flow pattern on the flow map. Oddie *et al.* (2003) studied two and three-phase flows in a large (15 cm i.d.) and inclined pipe. Considering liquid-liquid flow only, flow pattern characterization and holdup data for only two different upward inclinations (+45 and +90, from the horizontal) are reported. A closer look at their experimental setup suggests that transition to dispersed flow could have been prematurely spotted, since almost no flow development length was left before the test section. Fairusov *et al.* (2000) carried out full-scale experiments and reported a single stratified to dispersed flow pattern transition in a horizontal pipeline carrying oil-water mixtures (36.35 cm i.d.). A more detailed and accurate flow pattern classification is given by Elseth (2001). This author employed more sophisticated experimental techniques (high-speed camera, LDA and gamma-ray densitometry) for the flow pattern characterization (Elseth defined basically 9 oil-water flow patterns, whereas Trallero only 6).

A few published studies deal with modeling of flow pattern transitions in liquid-liquid systems. Coming out directly from the classical and reliable modelling accomplished by Taitel' group (Barnea, 1991, Barnea and Taitel, 1993 and 1994), for gas-liquid stratified flow, Trallero (1995) investigated the transition from horizontal liquid-liquid stratified flow based on the Kelvin-Helmholtz stability analysis of the interface for one-dimensional two-phase flow. That author proposed the Inviscid Kelvin-Helmholtz (IKH) analysis and the Viscous Kelvin-Helmholtz (VKH) analysis, the latter including the shear stresses. Equivalent criteria can be obtained based on the linear stability analysis and the well-posedness analysis of the system of hyperbolic equations of the two-fluid model of stratified flow. Brauner and Maron (1992a and 1992b) proposed the zero-neutral-stability (ZNS) condition and the zero-real-characteristics (ZRC) condition. The VKH condition and the ZNS condition are equivalent for long wave length systems, i.e, with zero surface tension effect. Finally, the one-dimensional wave model for incompressible flow provides similar transition criteria; however, it has been applied for gas-liquid systems only (Wallis, 1969, Crowley *et al.*, 1992 and 1993).

The first step to developing the proposed inverted production-logging technique is the direct modeling, i.e. a suitable flow-pattern-dependent model for holdup and pressure gradient has to be developed. Obviously, the better the direct modeling, the better the inverse mode predictions. In this work we propose a more complete stratified-to-dispersed-flow transition boundary based on a linear stability analysis. The exact solution of the linearized problem was developed according to the solution methodology presented by Whitham (1974). The oil and water velocity profiles in stratified flow were modeled via an adjusted Couette-Poiseuille profile; hence it was possible to access for a typical case the kinetic energy coefficients over all ranges of oil and water flow rates. The theory herein proposed considers also as relevant the viscosity-induced instability in stratified oil-water flow, so that intermediate waves can play a role in the force balance at the interface (Miesen *et al.*, 1992, Hu and Patankar, 1995, Bai, 1995). The long wave approximation is no longer applied so that a new destabilizing cross-section term is for the first time included in the model. The study of new closure relations for stratified flow is in order (Ullmann *et al.*, 2004, Ullmann and Brauner, 2006). A new closure relation for the interfacial shear stress, which accounts for an interfacial wavy structure, is suggested for the two-fluid model for stratified pipe flow and significant improvements in the pressure loss predictions are achieved. On the other hand, the new approach allows for the inclusion of the stabilizing surface tension term, normally set to zero (Trallero, 1995, Brauner and Maron, 1992a, Crowley *et al.*, 1993). The new transition boundary is compared with data from the literature as well as with the Trallero's VKH and IKH transition boundaries and Brauner's (2001) dispersed flow boundary. The transition criterion is then compared with new flow-pattern data collected on a horizontal and slightly inclined (-5$^o$, -2$^o$, -1.5$^o$, +1$^o$, +2$^o$ and +5$^o$) pipe flow.

## 2. Experimental Work

The experiments reported in this paper were performed at the Multiphase Test Facility of Shell Exploration and Production B.V., Rijswijk. Oil (Shell Vitrea 10, average density of 830 kg/m$^3$ and viscosity of 7.5 mPa.s)-water (brine, average density of 1060 kg/m$^3$ and viscosity of 0.8 mPa.s) flow was investigated in a 8.28 cm i.d. 15.5-meter long stainless steel pipe (pipe roughness 4.5x10$^{-5}$, oil-water interfacial tension of 0.0204 N/m). At the 15.5 m-long test section there was a 1.15 m-long transparent Perspex pipe section for visualizations. In between the mixing section and the test section a length of 250 D was left for the two-phase flow development. The test section was fixed to a table that could be pneumatically deviated from horizontal.

Video recording (Sony digital video recorder DSR-20P, tapes Sony ME DVM60) together with gamma-ray densitometry (density meter Berthold LB 444) were used for the flow pattern identification. Such technique allowed for more detailed flow pattern classification. It was possible to split the basic flow patterns shown in Rodriguez and Oliemans (2006) into sub-patterns. Data were collected for horizontal and slightly inclined flow (-5$^o$, -2$^o$, -1.5$^o$, +1$^o$, +2$^o$ and +5$^o$). The ranges of oil and water flow rates covered were 0.39 to 58.41 m$^3$/h and 0.31 to 48.54 m$^3$/h, respectively. Therefore, the mixture velocities varied from 0.04 m/s to 5.55 m/s. The total experimental data set consists of 296 points. The reference measurements, which include single-phase flow rates, densities and viscosities of the phases, pressures and temperatures, presented an uncertainty of 0.1% of range. The reader is referred to Rodriguez and Oliemans (2006) for a more detailed description of the multiphase flow setup and experimental techniques.

Stable interface waves of intermediate wave length, $\lambda$, were detected in upward and downward flow. A movie-recording section consisting of a Perspex rectangular box filled with water was built around the Perspex tube. The wave lengths were determined from image analysis of the digitized pictures taken from the recorded movies. The measurements were made possible with the help of homemade software developed in LabView® for the image acquisition and treatment (Fig. 1a).

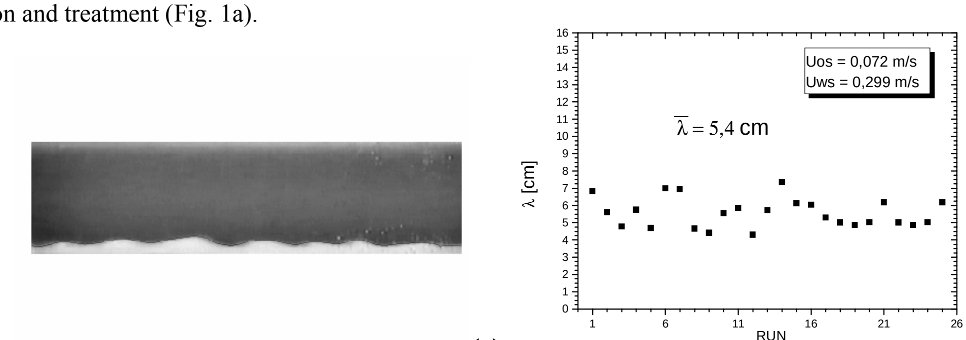


**(a)** **(b)**

Figure 1. (a) Interfacial wave detected via software; (b) wave length measurements.

Ten pictures were taken for each run and several measurements were made for each picture. A statistical procedure was carried out and the wave length data were found to follow a Gaussian distribution with time (Fig. 1b). Although the rectangular water box helped minimize image distortion, lens effects still needed to be corrected. This was accomplished by inserting a scale in the test section filled with water. The scale's length was then compared with another scale placed outside on the water box.

**3. Stability criterion and analysis**

The analysis is based on the two-fluid model of stratified flow (Fig. 2), where the area-averaged unsteady one-dimensional momentum and continuity equations are applied to both water and oil phases. The equations are then coupled through appropriated constitutive relations. The fluids are considered incompressible and the flow isothermal and without phase change.

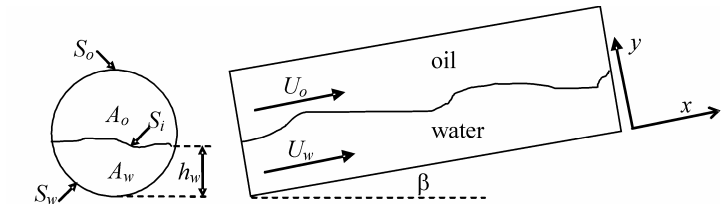


Figure 2. Schematic description of the stratified flow configuration.

*Continuity:*

$$\frac{\partial h_w}{\partial t}+U_w\frac{\partial h_w}{\partial x}+\frac{A_w}{A'_w}\frac{\partial U_w}{\partial x}=0 \quad , \quad \frac{\partial h_w}{\partial t}+U_o\frac{\partial h_w}{\partial x}-\frac{A_o}{A'_w}\frac{\partial U_o}{\partial x}=0 \tag{1),(2}$$

*Momentum:*

$$\rho_w\frac{\partial U_w}{\partial t}-\rho_o\frac{\partial U_o}{\partial t}+\rho_w U_w\left(k_w\frac{\partial U_w}{\partial x}+U_w\frac{dk_w}{dh_w}\frac{\partial h_w}{\partial x}\right)-\rho_o U_o\left(k_o\frac{\partial U_o}{\partial x}+U_o\frac{dk_o}{dh_w}\frac{\partial h_w}{\partial x}\right)+$$
$$+(\rho_w-\rho_o)g\cos\beta\frac{\partial h_w}{\partial x}+\frac{\partial(P_{iw}-P_{io})}{\partial x}=-\frac{\tau_w S_w}{A_w}+\frac{\tau_o S_o}{A_o}\pm\tau_i S_i\left(\frac{1}{A_w}+\frac{1}{A_o}\right)-(\rho_w-\rho_o)g\sin\beta \tag{3}$$

where $U$ corresponds to the average axial velocities, $\rho$ to the densities; $D$ is the internal diameter of the pipe; $g$ is the gravitational acceleration; $A_o$ and $A_w$ are the oil and water cross-sectional areas, respectively; $\tau_i$ and $\tau_w$ are, respectively, the interfacial and pipe wall shear stresses, $A_w = A_w(h_w)$ and $A'_w = dA_w/dh_w$. The kinetic energy distribution coefficients, $k_n$, are given by:

$$k_n=\frac{\langle u_n^2\rangle}{U_n^2}=\frac{1}{A_nU_n^2}\int_0^{A_n}u_n^2dA_n \tag{4}$$

where subscript $n$ is the phase index, $u_n$ corresponds to the velocity profile and the sign of the interfacial shear stress depends on which phase is flowing faster. Finally, the axial average pressure force change can be expressed in terms of the pressure level at the interface, $y = h_w$. A constitutive relation is necessary to close the problem. The Laplace-Young law is chosen in order to relate the pressures in the phases through the interfacial tension. The following relation is proposed, which includes both principal radii of curvature of the interface:

$$\frac{\partial(P_{io}-P_{iw})}{\partial x}=-\sigma\frac{\partial}{\partial x}\left(\frac{1}{h_w}\frac{\partial}{\partial h_w}\left\{h_w\left[1+\left(\frac{\partial h_w}{\partial x}\right)^2\right]^{-1/2}\right\}\right)=\sigma\frac{\partial}{\partial x}\left[\frac{1}{r_1(h_w)}+\frac{1}{r_2(h_w)}\right] \tag{5}$$

Introducing the sheltering hypothesis contribution (in Eq. 7), as indicated by Trallero (1995), and substituting Eq. (5) into Eq. (3), gives after some rearranging the area-averaged one-dimensional momentum equation for oil-water stratified flow. Together with Eqs. (1) and (2) this forms a set of 3 equations involving the 3 unknown variables, $U_w$, $U_o$ and $h_w$:

$$\rho_w \frac{\partial U_w}{\partial t} - \rho_o \frac{\partial U_o}{\partial t} + \rho_w U_w \left( k_w \frac{\partial U_w}{\partial x} + U_w \frac{dk_w}{dh_w} \frac{\partial h_w}{\partial x} \right) - \rho_o U_o \left( k_o \frac{\partial U_o}{\partial x} + U_o \frac{dk_o}{dh_w} \frac{\partial h_w}{\partial x} \right) + \\ + L \frac{\partial h_w}{\partial x} - \sigma \frac{\partial}{\partial x} \left[ \frac{1}{r_1(h_w)} + \frac{1}{r_2(h_w)} \right] = F \tag{6}$$

where

$$L = (\rho_w - \rho_o) g \cos\beta - \rho_f (U_w - U_o)^2 C_s S_i \left( \frac{1}{A_w} + \frac{1}{A_o} \right) \quad \text{and} \tag{7}$$

$$F = -\frac{\tau_w S_w}{A_w} + \frac{\tau_o S_o}{A_o} \pm \tau_i^o S_i \left( \frac{1}{A_w} + \frac{1}{A_o} \right) - (\rho_w - \rho_o) g \sin\beta \tag{8}$$

where the interfacial shear stress term, $\tau_i^o$, accounts for a smooth interface only, and the upper sign by the interfacial-stress term corresponds to oil flowing faster that water.

The hydrodynamic stability analysis comprises the study of the eventual increase of a small disturbance in the initial flow configuration, so that:

$$U_w = \overline{U}_w + \hat{U}_w; \quad U_o = \overline{U}_o + \hat{U}_o \quad \text{and} \quad h_w = \overline{h}_w + \hat{h}_w \tag{9}$$

where the superscript " ¯ " indicates the equilibrium condition (without disturbance) and $\hat{U}_w$, $\hat{U}_o$ and $\hat{h}_w$ represent the small disturbances imposed on the velocities and water level, respectively. Furthermore, $\overline{U}_w$, $\overline{U}_o$ e $\overline{h}_w$ are constants and $\hat{U}_w$, $\hat{U}_o$ and $\hat{h}_w$ are functions of {x,t}. According to the linear stability theory and following the method of small disturbances (Schlichting, 1979), $\hat{U}_w$, $\hat{U}_o$ and $\hat{h}_w$ are considered to be small and, therefore, second-order or higher terms can be neglected. Such simplification seems to be quite reasonably for the oil-water stratified flow, since the experimentally observed interfacial waves are relatively long or intermediate and do not present a turbulent behavior. Substituting Eq. (9) into Eqs. (1), (2) and (6) and neglecting all higher-order terms, results in:

$$\frac{\partial \hat{h}_w}{\partial t} + \overline{U}_w \frac{\partial \hat{h}_w}{\partial x} + \frac{\overline{A}_w}{\overline{A}'_w} \frac{\partial \hat{U}_w}{\partial x} = 0 \;, \qquad \frac{\partial \hat{h}_w}{\partial t} + \overline{U}_o \frac{\partial \hat{h}_w}{\partial x} - \frac{\overline{A}_o}{\overline{A}'_w} \frac{\partial \hat{U}_o}{\partial x} = 0 \;, \quad \text{and} \tag{10), (11}$$

$$\rho_w \frac{\partial \hat{U}_w}{\partial t} - \rho_o \frac{\partial \hat{U}_o}{\partial t} + \rho_w \overline{U}_w \left( k_w \frac{\partial \hat{U}_w}{\partial x} + \overline{U}_w \left.\frac{dk_w}{dh_w}\right|_{\overline{U}_w} \frac{\partial \hat{h}_w}{\partial x} \right) - \rho_o \overline{U}_o \left( k_o \frac{\partial \hat{U}_o}{\partial x} + \overline{U}_o \left.\frac{dk_o}{dh_w}\right|_{\overline{U}_o} \frac{\partial \hat{h}_w}{\partial x} \right) + \\ + \overline{L} \frac{\partial \hat{h}_w}{\partial x} - \sigma \left[ \frac{\partial^3 \hat{h}_w}{\partial x^3} + \frac{1}{\overline{h}_w^2} \frac{\partial \hat{h}_w}{\partial x} \right] = \partial \overline{F} \tag{12}$$

where the right-hand term of Eq. (12) is linearized through Taylor series expansion until the fist order. Note in the last LHS term of Eq. (12) the new cross-section curvature term. Eliminating $\hat{U}_w$ and $\hat{U}_o$ gives the differential equation for the disturbance or stability equation for oil-water stratified flow:

$$M \frac{\partial^4 \hat{h}_w}{\partial x^4} + N \frac{\partial^2 \hat{h}_w}{\partial t^2} + 2E \frac{\partial^2 \hat{h}_w}{\partial t \partial x} + F \frac{\partial^2 \hat{h}_w}{\partial x^2} + G \left( \frac{\partial \hat{h}_w}{\partial t} + H \frac{\partial \hat{h}_w}{\partial x} \right) = 0 \tag{13}$$

whose coefficients are:

$$M = \frac{A}{A'_w}\sigma \quad ; \qquad N = \left(\frac{\rho_w}{\overline{R}_w} + \frac{\rho_o}{\overline{R}_o}\right) \quad ; \qquad E = \frac{1}{2}\left[\frac{\rho_w \overline{U}_w}{\overline{R}_w}(1+k_w) + \frac{\rho_o \overline{U}_o}{\overline{R}_o}(1+k_o)\right] \;;$$

$$F = \frac{\rho_w \overline{U}_w^2}{\overline{R}_w}\left(k_w - \frac{A\overline{R}_w}{A'_w}\left.\frac{dk_w}{dh_w}\right|_{\overline{U}_w}\right) + \frac{\rho_o \overline{U}_o^2}{\overline{R}_w}\left(\frac{\overline{R}_w}{\overline{R}_o}k_o + \frac{A\overline{R}_w}{A'_w}\left.\frac{dk_o}{dh_w}\right|_{\overline{U}_o}\right) + \\ - \frac{A}{A'_w}\left[(\rho_w - \rho_o) g\cos\beta - \rho_f (U_w - U_o)^2 C_s S_i \left(\frac{1}{A_w} + \frac{1}{A_o}\right) - \frac{\sigma}{\overline{h}_w^2}\right] \;;$$

$$G = \frac{1}{\overline{R}_o}\left.\frac{\partial F}{\partial \overline{U}_o}\right|_{\overline{U}_w,\overline{h}_w} - \frac{1}{\overline{R}_w}\left.\frac{\partial F}{\partial \overline{U}_w}\right|_{\overline{U}_o,\overline{h}_w} \quad \text{and} \quad H = \frac{\frac{A}{A'_w}\left.\frac{\partial F}{\partial \overline{h}_w}\right|_{\overline{U}_w,\overline{U}_o} - \frac{\overline{U}_w}{\overline{R}_w}\left.\frac{\partial F}{\partial \overline{U}_w}\right|_{\overline{U}_o,\overline{h}_w} + \frac{\overline{U}_o}{\overline{R}_o}\left.\frac{\partial F}{\partial \overline{U}_o}\right|_{\overline{U}_w,\overline{h}_w}}{\frac{1}{\overline{R}_o}\left.\frac{\partial F}{\partial \overline{U}_o}\right|_{\overline{U}_w,\overline{h}_w} - \frac{1}{\overline{R}_w}\left.\frac{\partial F}{\partial \overline{U}_w}\right|_{\overline{U}_o,\overline{h}_w}} = c_o$$

where $c_o$ is the kinematic or continuity wave velocity, as deduced by Wallis (1969). Note that the inclusion of intermediate wave effects has a destabilizing character (last term of coefficient *F*).

The exact solution of the linearized problem was developed according to the solution methodology presented by Whitham (1974). The normal mode was used in order to analyze the ondulatory character of Eq. (13), so that:

$$\hat{h}_w(x,t) = \hat{h}_{w_{\max}} e^{i\mathbf{k}(x-ct)} \tag{14}$$

where $\mathbf{k} = 2\pi/\lambda$ is the wave number, $\lambda$ is the interfacial wave length and $c$ is the wave velocity. Substituting Eq. (14) into Eq. (13), gives the following equation:

$$\mathbf{k}\frac{N}{G}\left(c^2 - 2\frac{E}{N}c + \frac{F - M\mathbf{k}^2}{N}\right) + i(c - H) = 0 \tag{15}$$

Rearranging Eq. (15), using the Viète's theorem, replacing *H* by $c_o$ and approaching $c = c_1$ and $c = c_2$ gives:

$$w \cong \mathbf{k}c_1 - i\frac{G}{N}\frac{c_1 - c_o}{c_1 - c_2} \quad \text{and} \quad w \cong \mathbf{k}c_2 - i\frac{G}{N}\frac{c_2 - c_o}{c_2 - c_1} \tag{16), (17}$$

A necessary condition for the stability is that the imaginary component of *w* (Eqs. 16 and 17) must be negative, where *w* is the wave frequency. Rearranging Eqs. (16) and (17) and assuming that $c_1 > c_2$, the following criteria arise:

$$\begin{cases} 1 - G > 0 \\ 2 - c_1 \text{ and } c_2 \text{ must be real (Kelvin - Helmholtz analysis)} \\ 3 - c_2 \le c_o \le c_1 \end{cases} \tag{18}$$

where $V_o$ is the weighted average velocity, which corresponds to *E/N* as defined by Wallis (1969). The criteria shown above (Eq. 18) can be combined into one single criterion. Solving Eq. (15) for *c* (real component) and applying the criteria, results in the following general stability criterion:

$$0 \leq \frac{\left(\frac{c_o}{V_o}-1\right)^2}{1+\frac{M\left(\frac{2\pi}{\lambda}\right)^2-F}{NV_o^2}} \leq 1 \tag{19}$$

It is worthwhile to point out that the denominator of the expression shown above can be recognized as the Kelvin-Helmholtz's discriminator. It is in general satisfied for intermediate wave lengths through the interfacial tension. The validity of the presented criteria is to be tested using the experimental data.

### 3.1. Kinetic energy distribution coefficients

Brauner and Maron (1992a and 1992b) discussed the stabilizing effect of the distribution coefficients (or shape factors) on their inviscid ZRC condition. However, those authors only speculate over possible values and effects of the coefficients, and only for the lighter and more viscous phase. In order to assess on physical basis the effect of the distribution coefficient on the proposed general transition criteria (Eq. 19), we took the typical horizontal oil-water flow case studied by Elseth (2001). That author carried out a detailed scanning of the oil and water velocity profiles in stratified flow via a LDA technique. A simple model based on an adjusted velocity profile is proposed for the modeling of the oil and water kinetic energy distribution coefficients. We assume a Couette-Poiseuille profile for the water phase. The water level, $h_w$, and consequently the average water velocity, $U_w$ , are known quantities for every flow condition. $U_w$ is obtained from the solution of Eq. (8) for steady flow, as described in Rodriguez and Oliemans (2006). The average velocity can also be geometrically estimated using the following separated-flow approximation (refer to Fig. 2):

$$U_w = \frac{1}{\pi h_w^2}\int_0^{h_w} 2\pi(h_w - y)u_w(y)dy \tag{20}$$

We propose the following velocity profile:

$$u_w(y) = aU_m\left[\left(\frac{y}{h_w}\right)^{1/j_w} + bj_w\frac{y}{h_w}\left(1-\frac{y}{h_w}\right)\right] \tag{21}$$

where $U_m$ is the mixture velocity (= $U_{os}$ + $U_{ws}$, oil and water superficial velocities, respectively). The parameters *a* and *b* were adjusted to fit Elseth's data; results were: *a* = 1.25 and *b* = 0.06. Equation (20) is applied to adjust the parameter $j_w$ for each flow condition. An analogous procedure was adopted for the oil phase. Figure 3 shows a comparison between predicted velocity profiles and Elseth´s data for two different flow conditions.

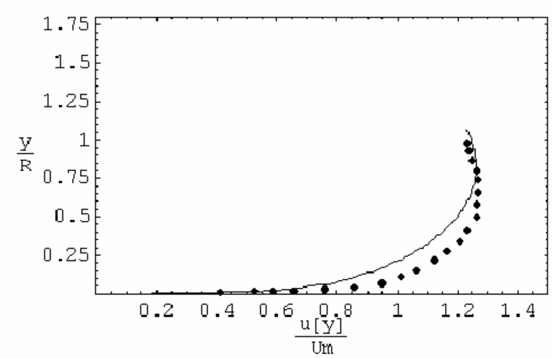


(a)

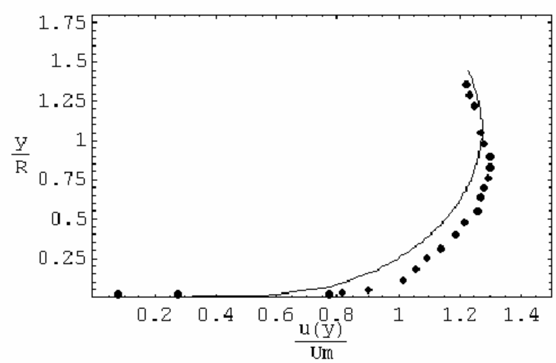


(b)

Figure 3. Present theory (solid curve) and Elseth´s (2001) data (dots); (a) oil velocity profile, $U_{ws}$ = 0,34 m/s and $U_{os}$ = 0.34 m/s; (b) water velocity profile, $U_{ws}$ = 0.765 m/s and $U_{os}$ = 0.255 m/s.

If one assumes that the velocity profiles are being reasonably well represented, the oil and water distribution coefficients, $k_o$ and $k_w$, respectively, can be readily estimated from Eq. (4) for every flow condition. Figure 4 shows the water distribution coefficient, $k_w$, as a function of oil superficial velocity for three different water superficial velocities. One may notice in Fig. 4 that $k_w$ can differ significantly from unity, i.e., even for the heavier and less viscous phase (water) the assumption of $k_w = 1$ is rather crude. $k_w$ deviates from the unity especially in the region of low water superficial velocities, $U_{ws}$, reaching values around 1.35. At low $U_{ws}$ the flow regime tends to laminar, therefore higher water kinetic-energy distribution parameters are expected. Another interesting finding is that $k_w$ never tends to unity, but converges to 1.04 at the lowest oil superficial velocities.

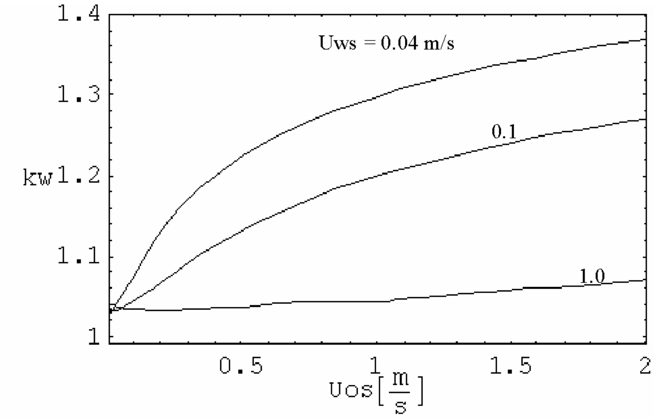


Figure 4. Water kinetic-energy distribution coefficient, $k_w$, as a function of oil superficial velocity, $U_{os}$, for water superficial velocities: $U_{ws}$ = 0.04 m/s, 0.1 m/s and 1.0 m/s.

### 3.3. Cross section curvature term and intermediate waves

According to Ullmann and Brauner (2006), in gas-liquid wavy stratified flow the interface curvature is dominated by secondary flows. Measurements of holdup and wetted perimeter in gas-liquid systems indicate extended wall wetting even in gravity dominated systems corresponding to large Eötvös numbers. This implies a concave rather than plane interface. We suggest the same phenomenon may also occur in liquid-liquid systems. The possible mechanisms may be: dragging of one phase by the other phase's secondary flows and/or pumping action due to lateral pressure gradient induced by the waves. The long wave approximation (Trallero, 1995, Brauner and Maron, 1992a and 1992b) is no longer applied in the pressure jump condition, Eq. (5). Therefore, a new destabilizing cross-section term naturally arises from the linearization process (last term of the wave coefficient $F$ of Eq. 19). Considering that the study of new closure relations for stratified flow is in order (Ullmann *et al.*, 2004, Ullmann and Brauner, 2006) a new closure relation for the interfacial shear stress is suggested for the two-fluid model for stratified pipe flow:

$$\tau_i = \tau_{i,smooth} + \tau_{i,wavy} = \tau_{i,smooth} + (\tau_{i,s} + \tau_{i,c}), \tag{22}$$

where $\tau_{i,smooth}$ considers only the interfacial friction when the interface is smooth, as shown in Rodriguez and Oliemans (2006) and the wave effects are incorporated into the model via $\tau_{i,wavy}$, which can be divided into the sheltering hypothesis term, $\tau_{i,s}$ (Trallero, 1995) and the herein proposed cross-section term, $\tau_{i,c}$. Therefore, the proposed interfacial-shear-stress closure relation is given by:

$$\tau_i = f_i \rho_f \frac{(U_w - U_o)|U_w - U_o|}{8} + \left[ C_s \rho_f (U_w - U_o)^2 + C_c \frac{\sigma}{h_w} \right] \frac{dh_w}{dx} \tag{23}$$

where $f_i$ and $\rho_f$ can assume either water or oil values accordingly to the holdup ratio (Rodriguez and Oliemans, 2006). The parameters $C_s$ and $C_c$ must be evaluated empirically; values determined on the data of this work were $C_s$ = 0.1 and $C_c$ = 1.5.

The new interfacial shear stress relation was applied and compared with the pressure loss data obtained in this work for horizontal stratified oil-water flow. Figure 5 shows model predictions and pressure gradient data as a function of the water superficial velocity for three oil superficial velocities. One may notice in Fig. 5 that a significant improvement was obtained by the inclusion of $\tau_{i,c}$. The commonly observed underestimation of the experimental data when applying the two-fluid model in the stratified flow region (Elseth, 2001, Rodriguez and Oliemans, 2006) is still observed, however it is diminished. The overall improvement in accuracy went from 31% to 22%. The best results were obtained within the region of low water and high oil superficial velocities. However, the two-fluid model seems to overestimates the experimental data for the lowest mixture velocities ($U_{os}$ = 0.07 m/s).

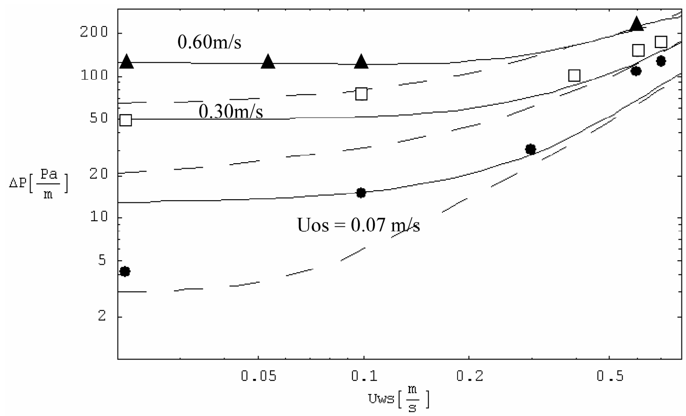


Figure 5. Pressure gradient data as a function of $U_{ws}$ for $U_{os}$ = 0.07 m/s, 0.30 m/s and 0.60 m/s; dashed curves, previous model; solid curves, the new model with $\tau_{i,c}$ .

The sort of instability that would generate intermediate waves is induced by tangential disturbances at the interface, rather than the inviscid Kelvin-Helmholtz instability. Viscous stratification has been recognized for a long time as possible cause of instability in liquid-liquid flow and it explains, in part, why the Kelvin-Helmholtz theory tends to overpredict the critical relative velocity for the initial generation of surface waves (Ishii, 1982). The original Kelvin-Helmholtz model refers to the flow of two inviscid fluids in relative motion (Drazin and Reid, 1981). When allowing viscous effects the relevance of the classical Kelvin-Helmholts analysis is no longer evident and instabilities of different nature, as viscosity-induced, may be preponderant. In that sense, the Viscous Kelvin-Helmholtz instalility theory is lacking. Furthermore, in the context of oil-water core-annular flow, it is believed that waves on the oil-water interface play a crucial role in the balance of forces acting on the oil core (Miesen *et al.*, 1992, Bai, 1995). The theory herein proposed states that in oil-water stratified wavy flow there would be a critical wave length, which would add an additional "rigidity" to the interface and delay the transition to dispersed flow.

## 4. Results and Discussion

### 4.1. Flow patterns

It is already known that the so-called dual-continuous flow patterns such as the Stratified with Mixing at the Interface (ST&MI) and the Stratified Wavy (SW) behave practically as pure stratified flow, in terms of slip and two-phase pressure loss (Rodriguez and Oliemans, 2006). Therefore, a single transition boundary separating all kinds of stratified flow patterns from the rest would be more suitable for practical purposes. The flow-pattern classification presented in Rodriguez and Oliemans (2006) was split out into more detailed sub-patterns of the basic flow patterns. Table 1 shows the new flow-pattern classification.

Table 1. Flow-patterns observed.

| Basic flow pattern | Sub-pattern |
|---|---|
| **ST** - Stratified Smooth | - |
| **SW** - Stratified Wavy | **SW_wl** – long wave |
| | **SW_wi** – intermediate wave |
| **ST&MI** - Stratified flow with mixing at the interface | **ST&MI_d** – only dispersion at the interface |
| | **ST&MI_wl** – dispersion and long wave at the interface |
| | **ST&MI_wi** - dispersion and intermediate wave at the interface |
| **Do/w&w** - Dispersion of oil in water and water | **Do/w&w_di** – discontinuous dispersion |
| | **Do/w&w_c** – continuous dispersion |
| **o/w** - Oil in water emulsion | - |
| **w/o** - Water in oil emulsion | **w/o_h** – homogeneous |
| | **w/o_in** – inhomogeneous |
| **Dw/o&Do/w** - Dispersions of water in oil and oil in water | - |

The classification was focused on the identification of a clear wavy structure, even when dispersion was present at the interface. Furthermore, when the wave length was a few times longer than the pipe diameter it was considered long wave. When it was of the order of the pipe diameter it was considered as intermediate wave.

### 4.2. Model comparisons and validation

The stratified-to-dispersed-flow transition boundary generated from the suggested general transition criterion, Eq. (19), is compared to Elseth's (2001) and the present flow-pattern data. Trallero's (1995) inviscid (IKH) and viscous (VKH) Kelvin-Helmholtz and Brauner's (2001) transition boundaries are also ploted onto the flow map for comparison (Fig. 6).

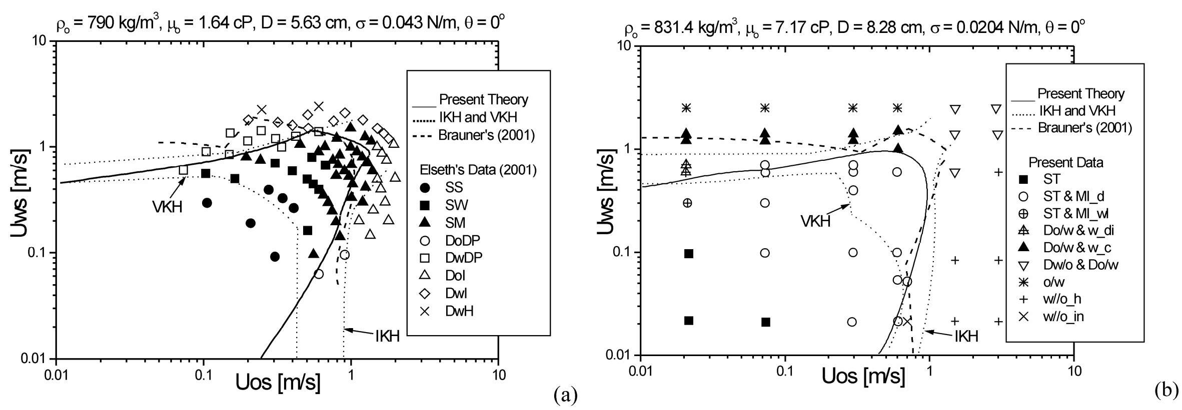


Figure 6. Present theory, Trallero's and Brauner's transition boundaries; (a) Elseth's data; (b) present data.

In Fig. 6a the present theory (solid curve) includes the modeling of the kinetic-energy distribution coefficients (Section 3.1) and the cross-section curvature term (Section 3.2). The presence of waves with wave lengths a few times longer than the pipe diameter was considered. One may see that at the region of high water-oil velocity ratio the VKH criterion underestimates, whereas the Brauner's criterion overestimates the experimentally observed stratified region (solid dots). The IKH and the proposed general criteria offer quite the same results and the best agreement with Elseth's data. At the region of similar water-oil velocity ratios Brauner's and present theory present similar results and good agreement with data; only VKH extremely underestimates the data. The IKH can generate no frontier by itself in that region of low relative velocity. Note at the low water-oil velocity ratio region the exclusion of the dispersed pattern DoDP, wrongly predicted as stratified by the IKH and Brauner's criteria. It seems that the general criterion works the best for extreme water-oil velocity ratios. Figure 6b shows a similar comparison, but now with the data generated in this work. Since it is not prudent to use the proposed velocity profile, Eq. (21), to other situations than Elseth's without further investigation, this time the distribution coefficients were made equal to unity. Once again the present theory agrees best with the data at the extreme velocity ratio regions. The VKH criterion showed similar results at those regions, but strongly underestimated the data in the other regions of the map. Brauner's and IKH criteria tend to overestimate the data, especially at the high water-oil velocity ratio region. Note that if the distribution coefficient effect had been considered, the stability region predicted by the general criterion would have been extended. That effect would have been more evident in the region of similar water-oil velocity ratios, probably matching Brauner's results in that region.

### 4.3. Effect of pipe inclination and the interfacial tension term

The validity of the general transition criterion for slightly inclined flow was tested using the experimental data collected in this work. Figure 7 shows the transition boundary predicted by the proposed criterion and the experimental flow map for -2° and -5° downward flow. The proposed transition criterion has a wave length-weighted interfacial tension term, as one may note in Eq. (19). Figure 7 shows the transition boundary obtained from Eq. (19) for a long wave case ($\lambda$ = 10 D, solid curve). In -2°-downward flow (Fig. 7a) the model predicts shrinkage of the stratified region mainly in the high water-oil velocity ratio region, in disagreement with experimental data. However, in that region a ST&MI_wi flow pattern was observed, i.e., an interfacial wave of the order of the pipe diameter was spotted. If a shorter wave length if applied in Eq. (19) the generated transition boundary can enclose all observed stratified-flow dots ($\lambda$ = D/4, dashed curve). In -5°-downward the predicted stratified region is significantly shrunk (Fig. 7b, solid curve). Again, waves of the order pipe diameter were observed at the high water-oil velocity ratio region (SW_wi and ST&MI_wi). If a shorter wave length is adopted a much better agreement with experimental data is observed (Fig. 7b, dashed curve). In downward flow the heavier phase is expected to speed up, while the lighter to accumulate in the pipe. This phenomenon is more evident in the high water-oil velocity ratio region, where the lighter and more viscous phase (oil) tends to accumulate due to viscous effects even in horizontal flow. Rodriguez and Oliemans (2006) have shown that in that region the water holdup can be 10 times as low as the injected water cut. A very low oil-water holdup ratio means a very high relative velocity. The transition criterion is sensitive to that source of instability, as shown in Fig. 7, but the data showed that there is still significant stratification. By analogy with gas-liquid flow, one may expect the existence of waves of intermediate wave length and high amplitude at the onset of transition from stratified to dispersed flow. The data confirm the existence of such waves (Fig. 7).

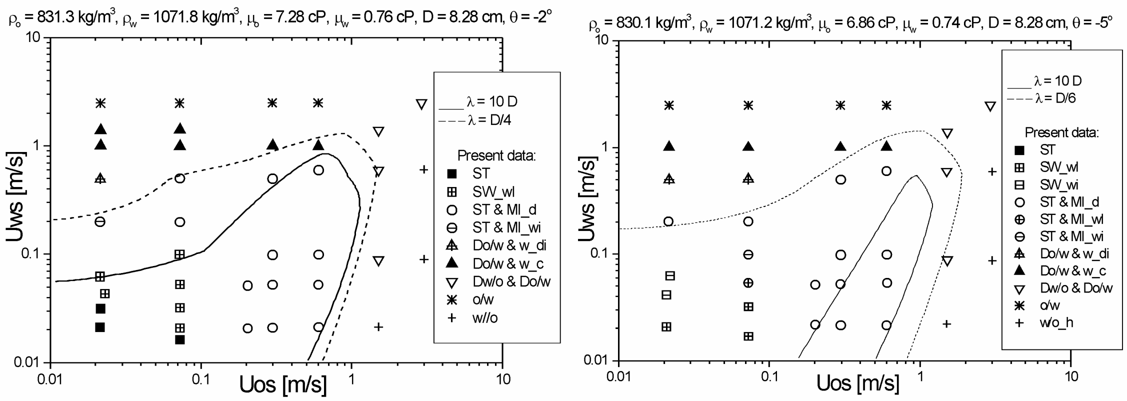


(a) (b)

Figure 7. General transition criterion and experimental flow map; (a) -2° and (b) -5° downward flow.

Figure 8 shows the predicted transition boundary and the experimental flow map for +2° and +5° upward flow. In +2°-upward flow (Fig. 8a) the model predicts shrinkage of the stratified region mainly in the low water-oil velocity ratio region, as expected since the heavier phase (water) now tends to slow down and accumulate in the pipe. However, the result is in disagreement with the experiments, although the ST&MI_wi and SW_wi flow patterns were observed, i.e., intermediate waves. Adopting a wave length of λ = D/4 (Fig 8a, dashed curve) the transition boundary encloses all observed stratified-flow dots. In +5°-upward the shrinkage of the stratified region is intensified (Fig. 8b, solid curve). Waves of the order pipe diameter were observed at the low water-oil velocity ratio region, as denoted by the ST&MI_wi flow pattern. Adopting a wave length of λ = D/5 (Fig 8b, dashed curve) promotes a better result. Note that two ST&MI_d dots were left outside the stratified region. A region of strong water backflow and recirculation was detected at low water and mid oil superficial velocities. The model herein proposed is not supposed to take those effects into account.

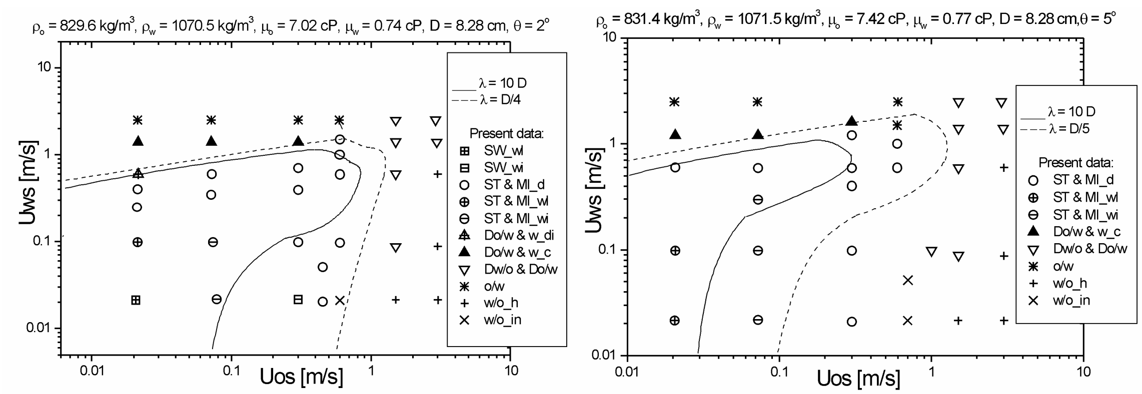


(a) (b)

Figure 8. General transition criterion and experimental flow map; (a) +2° and (b) +5° upward flow.

#### 4.4. Wave length measurements

Wave length data were automatically collected and treated via the homemade LabView® software. One may see in Table 2 that the wave length essentially diminishes with the increasing of either the holdup ratio ($C_w/\varepsilon_w$) or the inclination angle, which is in agreement with the instability theory herein discussed. Long and intermediate waves were spotted. Intermediate high-amplitude waves presented an averaged wave length that ranged from D/2 < λ < D. The averaged wave length included both high and low frequency wavy structures. If one computes only the high frequency waves, it is obtained an averaged minimum wave length of about $\lambda_s$ = D/2.2 (Table 2). Such results are in disagreement with the model predictions shown in Figs. 7 and 8, where waves of the order of D/4 led to the best agreements. New experiments with intrusive probes are required in order to verify if there would be even higher frequency waves. Waves on the cross section plane may also be spotted. An expression to account for the dependence of the wavelength with inclination angle is in development, which is to be incorporated into the proposed stability criterion.

Table 2. Interfacial wave length data.

| Inclination (degrees) | Test | $U_{os}$ (m/s) | $U_{ws}$ (m/s | $U_o$ (m/s) | $U_w$ (m/s) | $C_w/\varepsilon_w$ | D/λ | $D/\lambda_s$ |
|---|---|---|---|---|---|---|---|---|
| +5 | 1 | 0.072 | 0.021 | 0.25 | 0.03 | 0.32 | 1.6 | 2.2 |
| | 2 | 0.072 | 0.098 | 0.27 | 0.13 | 0.79 | 1.8 | 2.3 |
| | 3 | 0.072 | 0.296 | 0.33 | 0.38 | 1.03 | 1.8 | 2.2 |
| -5 | 4 | 0.021 | 0.041 | 0.02 | 0.46 | 7.35 | 2.0 | 2.2 |
| | 5 | 0.022 | 0.062 | 0.03 | 0.52 | 6.15 | 1.8 | 2.2 |
| | 6 | 0.072 | 0.099 | 0.08 | 0.66 | 3.87 | 1.6 | 2.2 |
| +2 | 7 | 0.078 | 0.022 | 0.22 | 0.03 | 0.34 | 1.8 | 2.1 |
| | 8 | 0.074 | 0.098 | 0.26 | 0.14 | 0.79 | 1.5 | 2.1 |
| -2 | 9 | 0.022 | 0.202 | 0.04 | 0.45 | 2.0 | 1.1 | -- |

## 5. Conclusions

A general stability criterion of liquid-liquid stratified flow based on the linear stability analysis is proposed. The exact solution of the linearized problem was developed according to the solution methodology presented by Whitham (1974). The stratified-to-dispersed-flow transition criterion should be equivalent to the Brauner's ZNS and Trallero's VKH conditions; however the model is more complete, since the modeling of the kinetic-energy distribution coefficients (or shape factors) and a new cross-section term are for the first time included. The oil and water velocity profiles in stratified flow were modeled via an adjusted Couette-Poiseuille profile; hence it was possible to access for a typical case the distribution coefficients over all ranges of oil and water flow rates. The theory herein proposed considers also as relevant the viscosity-induced instability in stratified oil-water flow, so that intermediate waves can play a role in the force balance at the interface. Therefore, the long wave approximation is no longer applied and the new destabilizing cross-section term naturally arises from the linearization procedure. A new closure relation for the interfacial shear stress is suggested for the two-fluid model for stratified pipe flow and significant improvement in the pressure loss predictions were achieved. On the other hand, the new approach allows for the inclusion of the stabilizing surface tension term, normally set to zero. The new transition boundary is compared with data from the literature as well as with the Trallero's VKH and IKH transition boundaries and Brauner's dispersed flow boundary. New oil-water flow pattern data collected in a 8.28 cm i.d. 15.5-meter long stainless steel pipe are offered. The transition criterion is then compared with experimental flow maps of horizontal and slightly inclined (-5$^o$, -2$^o$, +2$^o$ and +5$^o$) pipe flow. The following main conclusions can be drawn from this study:

1. The separated-flow approximation and the proposed Couette-Poiseuille profile provided a suitable representation of the velocity profiles experimentally observed by Elseth (2001).
2. The kinetic-energy distribution coefficients can deviate significantly from unity, even for the less viscous fluid (water); in fact, $k_w$ never tends to unity, but converges to 1.04 at the lowest oil superficial velocities and can reach 1.35 at the lowest water superficial velocities.
3. The new closure relation for interfacial shear stress intends to reflect a likely pressure loss related to secondary flows; by the inclusion of the new relation the commonly observed underestimation of the experimental data was significantly diminished (improvement in accuracy from 31% to 22%).
4. Nine sub-patterns originating from the basic flow patterns shown in Rodriguez and Oliemans (2006) were observed; the characterization was based on the observation of long and intermediate wavy structures.
5. New oil-water interface wave length data for four inclination from horizontal (-5, -2, +2, +5) are offered.
6. The proposed general stability criterion generated a single stratified-to-dispersed flow transition boundary that agreed very well with Elseth's data and the present data; the results were superior in comparison to Brauner's and Trallero's VKH and IKH transition boundaries, especially at extreme water-oil velocity ratios.
7. The proposed transition boundary is very sensitive to instability caused by high holdup ratios; it predicts shrinkage of the stratified area in the high water-oil velocity ratio region in downward flow and in the low water-oil velocity ratio region in upward flow; in those regions wavy structures were observed instead.
8. The incorporation of waves of intermediate wave length into the model produces better predictions, supporting the theory that intermediate waves would add an additional "rigidity" to the interface and delay the transition to dispersed flow; such waves were observed in our experiments.

## 6. Acknowledgements

The authors are grateful to Shell International Exploration and Production B.V. for supporting the experimental work. O. Rodriguez is grateful to FAPESP (Fundação de Amparo à Pesquisa do Estado de São Paulo, proc. 04/13374-7) for supporting his research at the University of São Paulo at São Carlos.

## 7. Reference list


Alkaya, B., Jayawardena, S.S., Brill, J.P., 2000. Oil water flow patterns in slightly inclined pipes. Proceedings of ETCE/OMAE2000 Joint Conference, New Orleans, February 14-17.

Angeli, P., Hewitt, G.F., 1998. Pressure gradient in horizontal liquid-liquid flows. International Journal of Multiphase Flow 24, 1183-1203.

Bai, R., 1995. Traveling waves in a high viscosity ratio and axisymmetric core annular flow. Ph.D. Thesis, University of Minnesota.

Bannwart, A.C., Rodriguez, O.M.H., de Carvalho, C.H.M., Wang, I.S., Obregon Vara, R.M., 2004. Flow patterns in heavy crude oil-water flow. Journal of Energy Resources Technology-Transactions of the ASME 126, 184-189.

Barnea, D. and Taitel, Y., 1994, Non-linear interfacial instability of separated flow, Chemical Engineering Science, v. 49, n. 14, 2341-2349.

Barnea, D., 1991. On the effect of viscosity on stability of stratified gas-liquid flow – Application to flow pattern transition at various pipe inclinations, Chemical Engineering Science, 46 (8), 2123-2131.

Barnea, D., Taitel, Y., 1993. Kelvin-Helmholtz stability criteria for stratified flow: viscous versus non-viscous (inviscid) approaches, International Journal of Multiphase Flow, 19 (4), 639-649.

Brauner, N., 2001. The prediction of dispersed flows boundaries in liquid/liquid and gas/liquid systems , Int. J. Multiphase Flow 27, 885-910.

Brauner, N., Maron, D.M., 1992a, Stability analysis of stratified liquid-liquid flow, International Journal of Multiphase Flow, v. 18, n. 1, 103.

Brauner, N., Maron, D.M., 1992b , Flow pattern transitions in two-phase liquid-liquid flow in horizontal tubes, International Journal of Multiphase Flow, v. 18, n. 1, 123.

Charles, M. E., Govier, G. W., Hodgson, G. W., 1961. The horizontal pipeline flow of equal density oil-water mixtures. Canadian Journal of Chemical Engineering 39 (1), 27-36.

Crowley, C.J., Wallis, G.B. and Barry, J.J., 1992 , Validation of a one-dimensional wave model for the stratified-to-slug flow regime transition, with consequences for wave growth and slug frequency, International Journal of Multiphase Flow, v. 18, n. 2, 249-271.

Crowley, C.J., Wallis, G.B. and Barry, J.J., 1993, Dimensionless form of a one-dimensional wave model for the stratified flow regime transition, International Journal of Multiphase Flow, v. 19, n. 2, 369-376.

Drazin, P.G., Reid, W.H., 1981. Hydrodynamic Stability. Cambridge University Press, Cambridge.

Elseth, G., 2001, An experimental study of oil-water flow in horizontal pipes, Ph.D. Thesis. The Norwegian University of Science and Technology.

Fairusov, Y.V., Arenas-Medina, P., Verdejo-Fierro, J. and Gonzales-Islas, R., 2000, Flow pattern transitions in horizontal pipelines carrying oil-water mixtures: full-scale experiments, Journal of Energy Resources Technology, v. 122, 169-175.

Flores, J.G., Chen, X.T., Sarica, C., Brill, J.P., 1997. Characterization of oil-water flow patterns in vertical and deviated wells. In: SPE Annual Technical Conference and Exhibition - SPE 38810, San Antonio, Texas.

Guet, S., O.M.H. Rodriguez, Oliemans, R.V.A., Brauner, N., 2006. Inverted dispersed multiphase flow models for liquid production rate predictions. International Journal of Multiphase Flow 32, 553-567.

Hu, H.H., Patankar, N., 1995. Nonaxisymmetric instability of core-annular flow. Journal of Fluid Mechanics 290, 231-224.

Ishii, M., 1982. Wave phenomena and two-phase flow instabilities. In: Handbook of Multiphase Systems by G. Hetsroni, McGraw-Hill, New York.

Lovick, J., Angeli, P., 2001. Two-phase liquid flows at the partially dispersed flow regime. Proceedings of 4th International Conference of Multiphase Flow – ICMF'01, New Orleans, May 27-June 1.

Lovick, J., Angeli, P., 2004. Experimental studies on the dual continuous flow pattern in oil–water flows. International Journal of Multiphase Flow 30, 139-157.

Miesen, R.H.M., Beijnon, G., Duijvestijn, P.E.M., Oliemans, R.V.A., Verheggen, T.M.M., 1992. Interfacial waves in core-annular flow. Journal of fluid Mechanics 238, 97-117.

Nädler, M., Mewes, D., 1997. Flow induced emulsification in the flow of two immiscible liquids in horizontal pipes. International Journal of Multiphase Flows 23, pp. 55-68.

Oddie, G., Shi, H., Durlofsky, L.J., Aziz, K., Pfeffer, B., Holmes, J.A., 2003. Experimental study of two and three phase flows in large diameter inclined pipes. International Journal of Multiphase Flow 29, 527-558.

Rodriguez, O.M.H, Mudde, R.F., Oliemans, R.V.A., 2004. Inversion of multiphase flow models for multiphase well logging: larger diameters and lightly inclined pipes. Proceedings of 4th North American Conference on Multiphase Technology, Banff, Canada, 3-4 June.

Rodriguez, O.M.H., Oliemans, R.V.A., 2006. Experimental study on oil-water flow in horizontal and slightly inclined pipes. International Journal of Multiphase Flow 32, 323-343.

Schlichting, H, 1979. Boundary-Layer Theory. McGraw-Hill, New York.

Sotgia G., and Tartarini P., 2001, Experimental and theoretical investigation on pressure drop reductions in oil water flows, 4th International Conference of Multiphase Flow, New Orleans, Lousiana, May 27-June 1.

Trallero J. L., 1995, Oil-water flow patterns in horizontal pipes, Ph.D. thesis, The University of Tulsa, Tulsa, Oklahoma.

Ullmann, A., Brauner, N., 2006. Closure relations for two-fluid models for two-phase stratified smooth and stratified wavy flows. International Journal of Multiphase Flow 32, 82-105.

Ullmann, A., Goldstein, A., Zamir, M., Brauner, N., 2004. Closure relations for the shear stresses in two-fluid models for laminar stratified flow. International Journal of Multiphase Flow, 30, 877-900.

Valle, A., Utvik, O.H., 1997. Pressure drop, flow pattern and slip for two-phase crude oil/water flow: experiments and model predictions. Proceedings of International Symposium on Liquid-Liquid Two Phase Flow and Transport Phenomena, Antalya, Turkey.

Wallis, G.B., 1969. One-Dimensional Two-Phase Flow. MacGraw-Hill, New York.

Whitham, G.B., 1974. Linear and Nonlinear Waves. John Wiley & Sons, New York.